International Journal of Research Publication and Reviews

Journal homepage: www.ijrpr.com ISSN 2582-7421

SYNTHESIS, CHARACTERIZATION AND ANTIMICROBIAL EVALUATION OF METAL II COMPLEXES DERIVED FROM *N*-HYDROXYBENZAMIDE DERIVATIVES

Kaltumbe B. M.[1], Fugu M. B.[1], Waziri I. B.[1], Yurari M. A.[2], Zannah B. D.[1] and Bute M. S.[1]

[1] Department of Pure and Applied Chemistry, Faculty of Physical Science, University of Maiduguri, Borno state.
kaltumbebabakura@unimaid.edu.ng
[2] Yobe State University, Department of Chemistry, Faculty of Science.

ABSTRACT :

Hydroxamic acids are part of the organic compounds known to have antimicrobial activities due to possession of biologically viable functional group (CONHOH), that plays an important role in forming therapeutic agents. In this study Hydroxamic acid ligands were synthesized by reacting 4-methoxybenzoylchloride and hydroxylamine hydrochloride. The synthesized ligands were complexed with metal (Mn (II) Co (II) and Ni (II)) salts of chloride in (1:1) molar ratio. These compounds were characterized by solubility, conductivity, melting point, elemental analysis (CHN and metal content), infrared (IR), UV-Vis, ^{1}H and ^{13}C NMR spectroscopies. From the infrared (IR) results, the complexes were coordinated to the metal via the oxygen of carbonyl and deprotonated hydroxyl oxygen (O,O) in bidentate manner. UV-Vis data revealed that, the geometry were octahedral and square planer. The compounds are air stable and soluble in protic solvents. The complexes were also formed in 1:2 (metal: ligand) ratio as confirmed by the microanalysis. The molar conductance suggested that all complexes are non-electrolytes due to the lower values observed. The antimicrobial study of the ligand and its metal complexes were assayed against five different micro-organisms which comprises of two Gram-positive bacteria (Staphylococcus aureus and Streptococcus pyogenes) and two gram-negative bacteria (Escherichia coli and Salmonella typhi) and one fungus (Candida albicans) and the results revealed that only the ligand (HL) and Ni (II) complex displayed significant activity. The free ligand (HL) displayed highest zone of inhibition against the bacteria tested, even though is less active than the compared antibiotics (ciprofloxacin and fluconazole) tested. Mn (II) and Co (II) complexes did not respond against organisms tested due insolubility of the compounds.

Keywords: CHARACTERIZATION, METAL II, N-HYDROXYBENZAMIDE, Synthesis,

Introduction

Hydroxamic acids are one of the most extensively studied chemical compounds due to their enormous applications in various fields. Hydroxamic acids have a biologically viable functional group of CONHOH, that plays an important role in forming therapeutic agents (Latifah *et al*., 2019). The compounds of hydroxamic acids can be presented as RC(O)NHOH and they are usually derived from oxoacids by replacing OH by NHOH and hydrocarbyl derivatives (Fugu, 2019). Therefore, Specific examples are named as *N*-hydroxy amides. They contain the oxime (NHOH) and the carbonyl (CO) groups as shown in Figure 1 below;

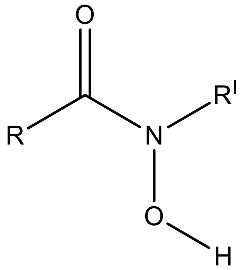

Figure 1: General structure of hydroxamic acid with R and R^I as organic residues (Fugu, 2019).

They are much weaker acids than the structurally related carboxylic acids RC(O)OH and produce hydroxamate ions (Elamin *et al*., 2021). The deprotonation could be either from the nitrogen or the oxygen, making them *N*-acids or *O*-acids. The hydroxamic acid imparts chelating properties to these acids and their *N*-substituted derivatives, which serve as bidentate di-oxygen ligands toward many metal ions such as Fe (III) and Cu (II). The complexes are highly coloured and are useful for the spectrophotometric and gravimetric analysis of the metal ions (Johann *et al*., 2019). Hydroxamate ions are best known as iron chelators, some hydroxamates are siderophores, which are compounds produced by microorganisms for the abstraction of iron from iron-deficient environments (Danah *et al*., 2020). Hydroxamate siderophores have been studied extensively due to their role as Fe (III) specific sequestering agents and potential pharmacological applications connected either with the microbial Fe(III) transport role or with the *in-vivo* decontamination of Fe(III) overload patients. Though the relationship between the biological effects and the strong chelating ability of hydroxamic acids is well established, very little is known about the metal complexes formed with natural cyclic monohydroxamic acids (Tripathi *et al.*, 2020). This is due to the decomposition of these compounds in solution and precipitation in the presence of metal ions such as Cu (II). Hydroxamic acids have particular affinities for hard cations such as Fe (III), Np (IV) and Pu (IV) with which they form five-membered chelate rings (Kakkar *et al.*, 2013). The chelating ability of hydroxamic acids has been used to link pharmaceutically useful ions such as radioactive or paramagnetic ions to monoclonal antibodies that direct the ion to a desired target tissue for tumour or tissue imaging or therapy purposes (Kahn, 2000). The use of hydroxamate coordination polymers as molecular magnets has also been explored (Fugu et al., 2021). Due to all these applications, the coordination chemistry of hydroxamates has evoked much interest (Marmion *et al.*, 2004). A variety of hydroxamic acid derivatives have recently been touted for their potential use as inhibitors of hypertension, tumour growth, inflammation, infectious agents, asthma, arthritis, and more (Brown *et al.*, 2001). Other biological applications include inhibition of enzymes such as prostaglandin H synthase, peroxidases, ureases, and matrix metalloproteinases (MMPs) which degrade the barriers holding cells in place and are involved in tumour growth (Gaynor *et al.*, 2001). The length of the carbon chain and the kind of acyl group give individual hydroxamic acids their unique characteristics. Hydroxamic acids are categorized as follows based on the length of the carbon chain.

Classification of Hydroxamic acids

i. Short-chain Hydroxamic acids

The carbon chain of short-chain hydroxamic acids is C_2-C_3. These are readily soluble in water, although some hydroxamic acids with significant chelating characteristics, such as acetohydroxamic acid and propionohydroxamic acid are utilized in resin manufacturing (Sharma *et al.*, 2012).

ii. Middle-chain Hydroxamic acids

Hydroxamic acids with a middle carbon chain range from C_4 to C_8. Amino hydroxamic acids are typically what these are. These are extremely helpful in the medical field because they are utilized to inhibit certain metalloproteases. It has been well established that hydroxamic acids such as butyrohydroxamic acid, Valero hydroxamic acid, succinyl hydroxamic acid, benzohydroxamic acid, nicotinoyl hydroxamic acid, homocysteine hydroxamic acid, suberoyl-anilidehydroxamic acid (SAHA), etc., and can be used in a variety of processes (Celine and Kelvin, 2000).

iii. Long-chain Hydroxamic acids

These are typically lengthy carbon chains with more than C_{12}. These are extremely effective at removing harmful metal ions from water because they are insoluble in water. Actinonin, mycobactin, phenylalanyl hydroxamic acid, lauryl hydroxamic acid, palmityl hydroxamic acid, etc., are utilized as surfactants in the detergent industry and also exhibit antibacterial and antifungal activity (Haron *et al.*, 2012).

Metal Complexes of Hydroxamic Acids

Hydroxamic acids have extraordinary complexing ability towards a very great number of metal ions because they have bi-dentate group (Jarvis *et at.*, 2023). The coloured and stable solutions of these metal complexes often provide spectrophotometric methods for determination of several metal ions. The complex formation between a metal M^+ and hydroxamic acid usually takes place with the replacement of the hydroxylamine hydrogen by the metal ion and ring closure through the carbon to oxygen to form the chelate (Tobias *et at.*, 2019). The complex formation usually takes place with the replacement of the hydroxylamine hydrogen by the metal ion and ring closure through the carbon oxygen as shown in the Scheme 1 below:

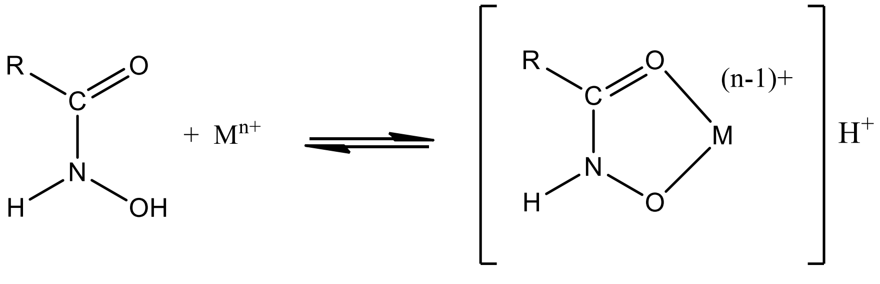

Scheme 1: formation of metal ion complexes.

All the metallic complexes of hydroxamic acids in which the *N*-hydrogen atom (N-H) is not replaced by any alkyl or aryl group are soluble in alkali showing acidic character of *N*-hydrogen atom (Sow *et al.*, 2023). The keto-form of hydroxamic acid contain one easily replaceable proton (mono-basic) while enol form may have two replaceable protons, thus behaving as a di-basic acid. The Keto-enol tautomerism provides a number of sites which are available for metal ion coordination (Fugu, 2019).

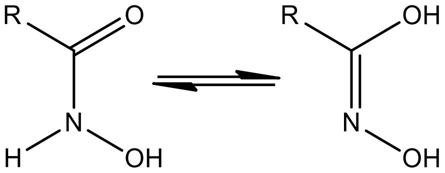

Figure 3: Keto-enol tautomer.

In general, hydroxamic acids form salts with almost all of the elements of group I, II, and III as well as the lanthanides and actinides group of the periodic table. The hydroxamic acid group behaves as a typical bi-dentate donor towards different metal ions. For instance, *N*-phenylbutyrohydroxamic acids and Cu (II), Ni (II), Zn (II), and Mn (II) create divalent metal chelates with a metal to ligand ratio of 1:2 (Abualreish *et al.*, 2014). The formula of these complexes is determined using a continuous variation approach. Denison developed the continuous variation method in relation to his research on the production of compounds in liquid mixtures. Job later used it to determine the formulas of the complexes generated in solutions by the reaction of two components using spectrophotometry.

The formation of many complex ions can be represented by the equation:

$$A + nB \longrightarrow ABn$$

Where A is a metallic ion, B may be either ion or molecule. To determine n, solutions of A and B of the same molar concentration are mixed in varying proportion and a suitable property of resulting solutions is measured (Abu-elnour, 1997).

Material and Method

All the reagents a chemicals and reagents used in this work were purchased from Sigma Aldrich through Ibra-Hadad Chemicals Limited and JB-Cays Chemicals; they were of analytical grade and were used without further purification. These include; 4-methoxybenzoylchloride ($CH_3OC_6H_4COCl$), hydroxylamine hydrochloride ($NH_2OH.HCl$), sodium hydroxide (NaOH), manganese (II) chloride tetrahydrate ($MnCl_2.4H_2O$), cobalt (II) chloride hexahydrate ($CoCl_2.6H_2O$), nickel (II) chloride hexahydrate ($NiCl_2.6H_2O$), methanol (CH_3OH), ethanol (C_2H_6O), acetone (C_3H_6O), benzene (C_6H_6), chloroform ($CHCl_3$), ethylacetate ($C_4H_8O_2$) and n-Hexane (C_6H_{14}). The melting points of the complexes were determined using Griffin melting point apparatus. Molar conductivity measurement (10-3 M solution in methanol) was obtained on the metler P163, while elemental analysis were carried out on a Perkin-Elmer model 2400 series 11CHNS/O elemental analyser. The metal content of the complexes was determined using AA240FS, Fast Sequential Atomic Absorption Spectrometer. The electronic absorption spectra of the complexes were obtained using UV-2550 Shimadu Spectrophotometer in the wavelength range of 250-800nm. The infrared (IR) spectra were recorded as NaBr disc on Perking Elmer 1310(IR) in the range of 4000-400cm-1. The antibacterial activity was determined using disc diffusion method.

Synthesis of 4-methoxybenzoylchloride Hydroxamic Acid Ligand

Hydroxamic acid ligand was synthesized using the procedure described by Latifah *et al.*, (2019) and by dissolving hydroxylamine hydrochloride (2.57 g, 37.0 mmol, 1 eq) in 30 mL ethylacetate and this was added into a stirring cold solution containing sodium hydroxide and ice (7.4 g, 185.0 mmol, 5 eq and 30 g) respectively. The solution was allowed to stir at room temperature (r.t) for 15 minutes to complete dissolution. The aroyl chlorides (4-methoxybenzoylchloride; 6.24 g, 37.0 mmol, 1 eq) was dissolved separately in 10 mL of ethylacetate added wisely in drops for 5 minutes. The solution was allowed to stir for further 15 minutes and form two layers, an organic layer and aqueous layer. The organic layer is the portion of interest and was collected using separating funnel and it was dried in a desiccator under anhydrous calcium chloride for further analysis. The reaction path way for the synthesis is shown schematically in **Scheme 2.**

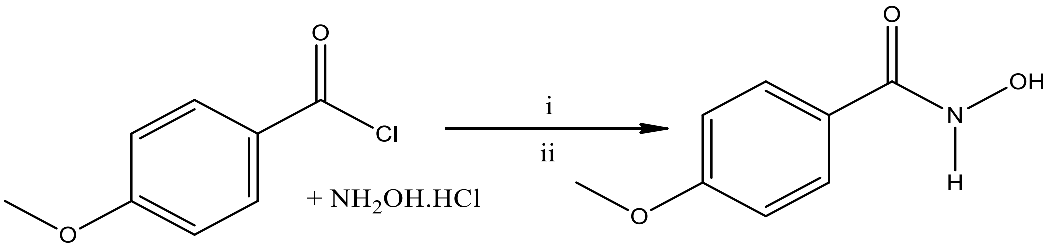

Where; i = NaOH/ethylacetate; ii = ice, r.t for 30 minutes

Scheme 2: Synthesis of 4-methoxybenzoylchloride Hydroxamic acid ligand.

Synthesis of Metal Complexes of 4-methoxylbenzoylchloride Hydroxamic Acid Ligand

Hydroxamic acid metal complexes were synthesized using the procedure described by Fugu, (2019). The synthesized ligand HL (0.25 g, 1.3 mmol) was dissolved in 30 mL of methanol. The methanolic solution of the ligand was added to a stirring solution of the metal salts; [$MnCl_2.4H_2O$ (0.22 g, 1.3 mmol) $CoCl_2.6H_2O$ (0.18 g, 1.1 mmol) and $NiCl_2.6H2O$ (0.18 g, 1.1 mmol)] each in 30 mL of methanol, followed by the addition of sodium hydroxide (0.04 g, 1.0 mmol) and stir for 3 hours. The product formed were filtered and allowed to evaporate under reduced pressure. The final products (complexes) were weight and the percentage yields were calculated using standard procedure. The scheme for the synthesis is shown below;

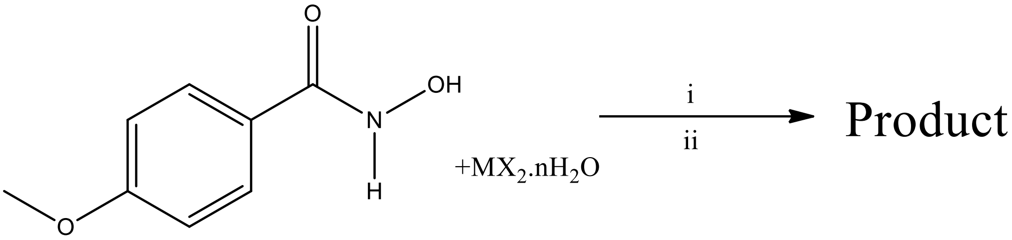

M = Mn (II), Co (II) and Ni (II) X= Cl; n = 2, 4 or 6, i = MeOH/NaOH; ii = r.t for 3hrs

Scheme 3: Synthesis of the complexes of 4-methoxylbenzoylchloride.

Result and Discussion

Physicochemical Properties

The analytical data along with some physical properties are shown in Table 1. The ligands, **HL** on interaction with Mn (II), Co (II) and Ni (II) formed complexes with moderate yield (37-59 %) corresponding to the general formula $[M(L)_2(H_2O)_2]$, where M=Mn (II) Co (II) and $[M(L)_2]$, where M= Ni (II) and L= hydroxamic acid ligands. The compounds are air stable with sharp melting points ranging from 210-253 °C. The sharp melting points indicates that the complexes are probably pure (Fugu, 2019; Fugu *et al.*, 2019; Waziri, 2022; Waziri *et al.*, 2023). The molar conductivity (Λ_M) values for the complexes are in the range of 0 - 3.44×10^{-2} Scm^2mol^{-1} suggesting the non-electrolytic nature of the complexes in solutions (Temel, 2014). The colour of the free ligand is peach while those of complexes were brown and pale green.

Table 1: Physical characteristics and data for the Hydroxamic Acid Ligand and its Metal Complexes.

Compounds	Molecular formula/Molar mass (g/mol)	Colours	Melting point (°C)	Yield (%)	Molar conductivity (Scm^2mol^{-1})
HL	$C_8H_9NO_3$ (167.16)	Peach	210	57	-
$[Mn(L)_2(H_2O)_2]$	$Mn(C_{16}H_{20}N_2O_8)$ (423.28)	Brown	227	59	1.20
$[Co(L)_2(H_2O)_2]$	$Co(C_{16}H_{20}N_2O_8)$ (427.27)	Brown	248	37	0.99
$[Ni(L)_2]$	$Ni(C_{16}H_{16}N_2O_6)$ (391.00)	Pale green	253	49	1.34

HL = 4-methoxy-*N*-hydroxybenzamide

The solubility of the Ligand and its Metal Complexes

The solubility of the compounds was carried out using polar and non-polar solvents: such as distilled water (H_2O), methanol (CH_4O), ethanol (C_2H_6O), acetone (C_3H_6O), benzene (C_6H_6), chloroform ($CHCl_3$), ethyl-acetate ($C_4H_8O_2$) and n-hexane (C_6H_{14}) presented in Table 2. The ligand was insoluble in distilled water and soluble in methanol, ethanol, also, slightly soluble in acetone, chloroform ($CHCl_3$), and ethyl-acetate ($C_4H_8O_2$) and insoluble in benzene (C_6H_6), and n-Hexane. The complexes are soluble in methanol (CH_3OH), ethanol (C_2H_6O), acetone (C_3H_6O) and ethyl-acetate ($C_4H_8O_2$), they are slightly soluble in distilled water (H_2O), chloroform ($CHCl_3$) and insoluble in n-Hexane and benzene (C_6H_6). These indicates that the compounds synthesized are probably polar.

Infrared Spectra

Infrared (IR) spectral studies can be used to determine the coordination modes of ligands toward metal ions. Infrared spectroscopy (IR) offers vital insights into chemical bonding and functional groups. The spectral shifting, disappearance and emergence of new bands in the complexes of Mn (II), Co (II) and Ni (II) of the ligand (**HL)** can be used to deduce the mode of coordination. Table 3 shows a list of the major infrared bands.

Table 2: The Solubility of the Ligand/Complexes.

Compounds	Distilled water		Methanol		Ethanol		Acetone		Ethyl acetate		Chloroform		n-Hexane		Benzene	
HL	IS	SS	S	S	S	S	SS	SS	SS	S	SS	SS	IS	SS	IS	IS
$[Mn(L)_2(H_2O)_2]$	IS	IS	SS	S	SS	S	IS	SS	SS	SS	IS	SS	IS	IS	IS	IS
$[Co(L)_2(H_2O)_2]$	IS	SS	SS	S	SS	S	SS	S	IS	IS	SS	S	IS	SS	IS	IS
$[Ni(L)_2]$	IS	IS	S	S	S	S	SS	S	SS	SS	SS	S	SS	SS	IS	IS

Note: c = cold solvent, h = hot solvent, s = soluble, ss = slightly soluble, is = insoluble

Table 3: Relevant Infrared Frequencies (cm^{-1}) of the Hydroxamic Acid Ligand and the Metal Complexes.

Compounds	v(N-H)	v(O-H)	v(C=O)	v(N-O)	v(M-O)
HL	3259	2930	1670	821	-
$[Mn(L)_2(H_2O)_2]$	3007	-	1672	846	443
$[Co(L)_2(H_2O)_2]$	3004	-	1686	826	417
$[Ni(L)_2]$	3011	-	1603	826	417

The bands assignment was based on the comparison with similar studies on hydroxamic acids ligands, mixed ligands complexes and some drug-based metal complexes (Chauhan *et al*., 2016; Chauhan *et al*., 2017; Fugu, 2019; Fugu *et al*., 2019, Latifah *et al*., 2018; Latifah *et al*., 2019; Waziri *et al*., 2014; Waziri, 2022; Waziri *et al*., 2023). The complexation had indeed occurred in a bidentate manner through the oxygen of the carbonyl (C=O) and deprotonated hydroxyl (OH) groups and the coordination mode suggested is *O,O* mode. The O-H bands which appeared in the region of 2930 cm^{-1} in the spectrum of **HL** disappeared in all the complexes due to deprotonation of the OH and coordination of oxygen from the hydroxyl group to the metal ion and this was confirmed by creating new bands around 417-443 cm^{-1} that suggest metal to oxygen bond (Latifah *et al*., 2018; Latifah *et al*., 2019;). Strong bands exhibiting N-H stretching vibrations was observed at 3259 cm^{-1} for ligand (**HL**). In their metal complexes, the N-H bands were present in all the spectra of the metal complexes due to not participation in the coordination. The sharp band ascribed to v(N-O) at 821 cm^{-1} in the spectra of **HL**, was shifted to higher wavenumbers (826) cm^{-1} in the complexes though it did not participate in the coordination (Chauhan *et al*., 2017). The shifting of v(C=O) bands in the spectra of the **HL** complexes indicating the involvement of carbonyl (C=O) group in complexation via oxygen atom. This is further supported by the appearance of new weak bands of (M-O) down 500 cm^{-1} in the spectra of complexes (Chauhan *et al*., 2016).

Electronic Spectra

The geometry of the complexes can be predicted from UV-Vis study. The UV-Vis spectra of the ligand **HL** and their metal complexes of Mn (II), Co (II) and Ni (II), were carried out at 10^{-3} M concentration in ethanol in the range of 50000-12500 cm^{-1}. The most absorption bands occurred on the spectra of free ligand **HL** consists of an intense band centred at 37594-43478 cm^{-1} as indicated in Table 4.

Table 4: Electronic Absorption Spectra Data for the Complexes.

Compounds	λ_{max}(nm)	Absorption (cm^{-1})	Band assignment	Geometry
HL	230	43478	$\pi \rightarrow \pi^*$	-
	266	37594	$n \rightarrow \pi^*$	
$[Mn(L)_2(H_2O)_2]$	241	41494	$^6A_1g \rightarrow {}^4Eg(D)$	Octahedral
	265	37736	$^6A_1g \rightarrow {}^4Eg(D)$	
	301	33223	$^6A_1g \rightarrow {}^4Eg(D)$	
$[Co(L)_2(H_2O)_2]$	235	42553	$^4T_1g \rightarrow {}^4T_1g(P)$	Octahedral
	251	39841	$^4T_1g \rightarrow {}^4T_1g(P)$	
	290	34483	$^4T_1g \rightarrow {}^4T_1g(P)$	
$[Ni(L)_2]$	237	42194	$^3A_2g \rightarrow {}^3T_1g(P)$	Square planer
	275	36364	$^3A_2g \rightarrow {}^3T_1g(P)$	
	320	31250	$^3A_2g \rightarrow {}^3T_1g(P)$	

The band assignments were based on the comparison with similar studies of (Saif *et al*., 2016; Mandeep, 2017; Ndahi *et al*., 2018; Waziri, 2022; Waziri *et al*., 2023). These bands were assignable to π→π* transition which is due to presence of Carbon to Carbon (C=C) found within the free ligand (Saif *et al*., 2016; Waziri, 2022; Waziri *et al*., 2023).

^{1}H NMR Spectra of the Ligand (HL)

The ^{1}H NMR spectrum of **HL** showed a singlet signal at 4.3 ppm associated with proton of the methoxy (OCH_3) group, two doublet signals at 7.8 and 7.4 ppm which were assigned to the aromatic protons. A singlet signals at 10.5 and 10.0 ppm correspond to protons belongs to NH and OH groups, respectively. Similar result reported by Fugu *et al*., (2019). The summarized information on the ^{1}H Nuclear Magnetic Resonance of the free ligands are presented in Table 5.

Table 5: ^{1}H NMR data of the Ligand (HL).

Compounds	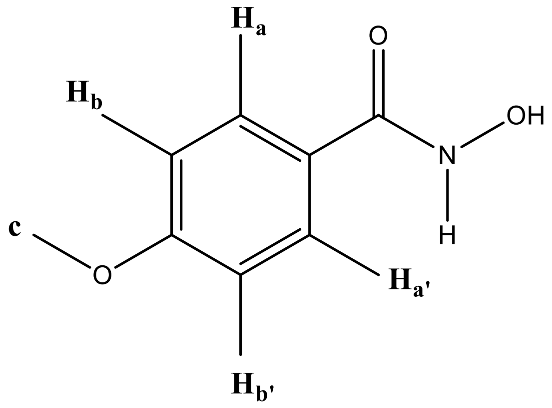				
Types of protons exist in the compounds (ppm)	Ha/Ha'	Hb/Hb'	O-H	N-H	Hc
HL	d (7.8)	d (7.4)	s (10.5)	s (10.0)	s (4.3)

d = doublet and s = singlet

^{13}C NMR Spectra of the Ligand (HL)

^{13}C NMR was used in determining the number of non-equivalent carbons and types of carbons that exists in the ligands. There are different types of carbons exists in the **HL** ligand; the carbonyl (C=O) carbon, aromatic carbons (Ar-C), and methoxy (OCH_3) carbon. The carbonyl (C=O) signals appeared at 154.8 and 161.1 ppm for **HL**. The aromatic carbon for **HL** appeared at 114.3, 119.7 ppm while the methoxy carbon appeared at 55.2 ppm similar results were reported by (Waziri, 2022; Waziri *et al*., 2023). The summarized information on the ^{13}C Nuclear Magnetic Resonance of the free ligand is presented in Table 6.

Table 6: ^{13}C NMR data of Ligand (HL)

Compound	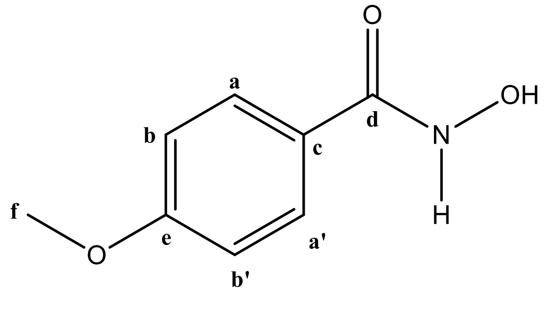					
Types of carbons exist in the compounds (ppm)	$C_a/C_{a'}$	$C_b/C_{b'}$	C_c	C_d	C_e	C_f
HL	114.3	119.7	129.4	161.1	163.4	55.8

Microanalysis

The percentage of the C, H, N and the metal estimation data of the hydroxamic acid ligand and the metal complexes are presented in table 7. The microanalysis of the compounds was presented in Table 7. The results revealed that the percentage (%) of C, H, N and metal content are in good agreement with the proposed structures from the data obtained. The metal ion percentage also agrees with proposed structures.

Table 7: Microanalysis Data.

Compounds	Molecular formula (Molar mass)	Microanalysis, % Calculated (found)			
		C	H	N	M
HL	$C_8H_9NO_3$ (167.16)	57.48 (56.92)	5.43 (5.28)	8.38 (8.28)	-
$[Mn(L)_2(H_2O)_2]$	$Mn(C_{16}H_{20}N_2O_8)$ (423.28)	47.44 (47.21)	5.31 (5.23)	6.15 (6.08)	12.26 (12.18)
$[Co(L)_2(H_2O)_2]$	$Co(C_{16}H_{20}N_2O_8)$ (427.27)	45.40 (45.23)	4.76 (4.66)	6.62 (6.49)	12.98 (12.87)
$[Ni(L)_2]$	$Ni(C_{16}H_{16}N_2O_6)$ (391.00)	44.98 (44.77)	4.72 (4.61)	6.56 (6.46)	13.79 (13.61)

C = Carbon, H = Hydrogen, N = Nitrogen, M = Metal

Based on the microanalysis data and spectroscopic studies above the following structures were proposed for the complexes shown:

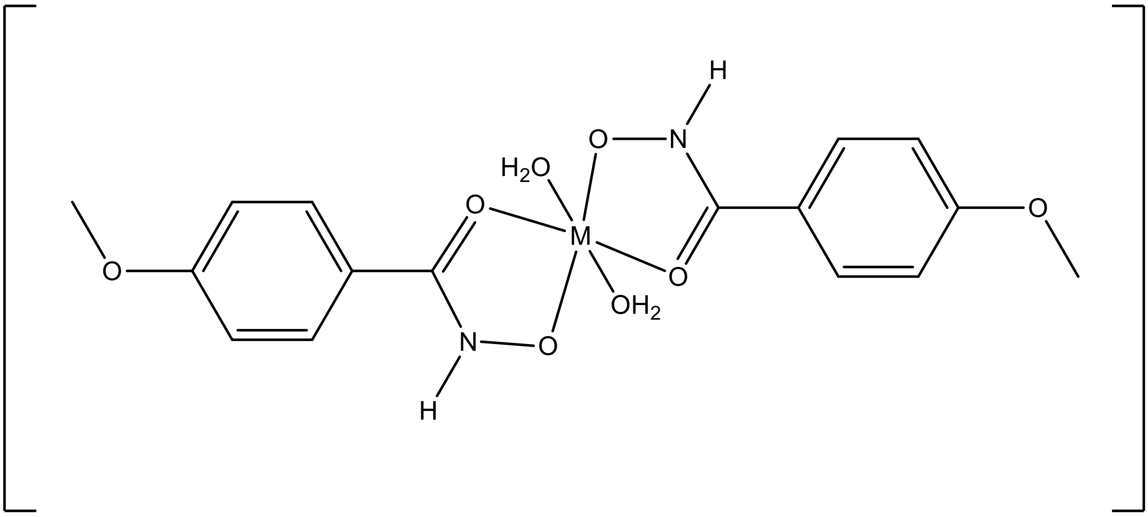

Where M = Mn (II) and Co (II)

Propose structure of $M(L)_2(H_2O)_2$ metal complexes.

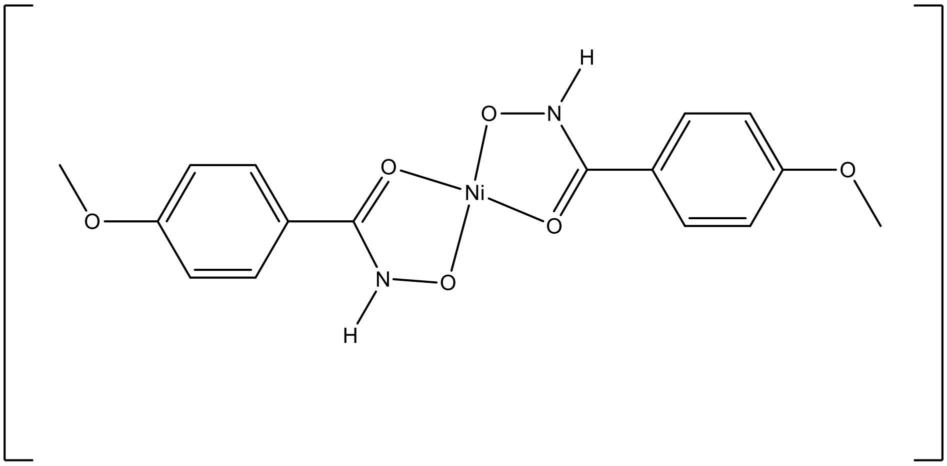

Propose structure of $Ni(L)_2$ complex.

Antimicrobial Activities of the Ligand (HL) and the Metal Complexes

The antimicrobial studies for the **HL** and its Complexes were tested against five different micro-organism which comprises of two Gram-positive bacteria (*Staphylococcus aureus* and *Streptococcus pyogene*), and two Gram-negative bacteria (*Escherichia coli and Salmonella typhi*) and one fungus (*Candida albicans*) at three different concentrations (30, 20 and 10 µg/mL). The results of the inhibition zones are presented in Table 8.

Table 8: Antimicrobial Activities of the Ligand (HL) and Metal Complexes.

Compounds	Concentrations (µg/mL)	Inhibition zone, mm (Mean ± SD)				
		S. aureus	*S. pyogenes*	*S. typhi*	*E. coli*	*C. albicans*
HL	30	25.0±0.00	0.00±0.00	0.00±0.00	0.00±0.00	0.00±0.00
	20	20.0±0.00	0.00±0.00	0.00±0.00	0.00±0.00	0.00±0.00
	10	15.0±0.00	0.00±0.00	0.00±0.00	0.00±0.00	0.00±0.00
$[Mn(L)_2(H_2O)_2]$	30	0.00±0.00	0.00±0.00	0.00±0.00	0.00±0.00	0.00±0.00
	20	0.00±0.00	0.00±0.00	0.00±0.00	0.00±0.00	0.00±0.00
	10	0.00±0.00	0.00±0.00	0.00±0.00	0.00±0.00	0.00±0.00
$[Co(L)_2(H_2O)_2]$	30	0.00±0.00	0.00±0.00	0.00±0.00	0.00±0.00	0.00±0.00
	20	0.00±0.00	0.00±0.00	0.00±0.00	0.00±0.00	0.00±0.00
	10	0.00±0.00	0.00±0.00	0.00±0.00	0.00±0.00	0.00±0.00
$[Ni (L)_2]$	30	13.0±0.00	0.00±0.00	0.00±0.00	0.00±0.00	0.00±0.00
	20	8.00±0.00	0.00±0.00	0.00±0.00	0.00±0.00	0.00±0.00
	10	0.00±0.00	0.00±0.00	0.00±0.00	0.00±0.00	0.00±0.00
Controls						
Ciprofloxacin	30	34.33±0.33	33.33±0.33	34.33±0.33	33.33±0.33	
	20	31.33±0.33	31.33±0.33	31.33±0.33	31.33±0.33	
	10	28.00±0.33	26.00±0.33	29.00±0.33	28.00±0.33	
Fluconazole	30					29.77±0.23
	20					26.77±0.23
	10					24.77±0.23

The values are presented as mean±SEM

KEYS: *S. aureus=Staphylococcus aureus, S. pyogenes=Streptococcus pyogenes, S.=Salmonella typhi, E. coli=Escherichia coli* and *C. albicans=Candida albicans*

The free ligand **HL** displayed zone of inhibition of 25 mm at 30 µg/mL, 20 mm at 20 µg/mL and 15 mm at 10 µg/mL against *S. aureus*. The Ni (II) complex of the **HL** displayed inhibition zone of 13 mm at 30 µg/mL and 8 mm at 20 µg/mL concentrations against *S. aureus* while Mn (II) and Co (II) complex of **HL** showed no zone of inhibition at concentrations tested. This result is in line with a result reported by Waziri *et al*., (2014); Ndahi *et al*., (2015); Ndahi *et al*., (2018); Rafiee *et al*., (2014). The inactivity of Mn (II) and Co (II) complexes against the micro-organism may be due to insolubility of the compounds. These compounds could be possibly used as disinfectant at high concentrations as reported by Pepeljnjak *et al*., (2005).

The Minimum Inhibitory Concentration (MIC)

The MIC of the free ligand **HL** was tested because it is the only compound that displayed an appreciable zone of inhibition against *Staphylococcus aureus* at all the concentrations tested. The MIC was tested using concentrations of 10, 8, 6, 4, and 2 µg/mL and the result revealed that the minimum inhibitory concentration that showed visible growth is at 4 µg/mL.

The Minimum Bactericidal Concentration (MBC)

The MBC of the free ligand **HL** was tested because it is the only compound that was used to determine the MIC. The MBC was tested using same concentrations of 10, 8, 6, 4, and 2 µg/mL as used in MIC determination and the result revealed that the minimum bactericidal concentration (MBC) that kills the organism is 6 µg/mL.

Table 9: The Minimum Inhibitory Concentration (MIC) of the Ligand HL

Compound	Conc. (μg/mL)	*S. aureus*
HL	10	S
	8	S
	6	S
	4	S
	2	R

HL = 4-methoxy-*N*-hydroxybenzamide, S = Susceptibility, R = Resistance.

Table 10: The Minimum Bactericidal Concentration (MBC) of the Ligand HL

Compound	Conc. (μg/mL)	*S. aureus*
HL	10	S
	8	S
	6	S
	4	R
	2	R

CONCLUSION :

In this work, new Hydroxamic acid ligand and its metal complexes of Mn (II), Co (II) and Ni (II) have been reported. The compounds have been characterized by solubility, conductivity, melting point, infrared, UV/Visible, microanalysis, and ^{1}H and ^{13}C NMR, and their antimicrobial potential have been tested. The compounds are air stable and soluble in most protic solvents which suggested that, they are probably polar compounds. Based on the physical analysis; the complexes have various colours, with high melting point and lower conductivity values that indicated their non-electrolytic nature. The complexes were formed in 1:2 (metal to ligand) molar ratio as confirmed by the microanalysis while the coordination of the ligands to the metal is through the deprotonated oxygen of the hydroxyl group and oxygen of the carbonyl group (i.e. *O,O*) as suggested by the infrared spectral data. The UV/Visible spectral band observed indicated that, the adopted geometry is either square planar or octahedral. The *in-vitro* antimicrobial study revealed that, the compound **HL** has the highest activity among the compounds although less active when compare to the control drugs (ciprofloxacin and fluconazole) tested.

REFERENCES :

Abu-elnour, S. H. (1997). Preparation and properties of n-phenylbutyrohydroxamic acid and n-p-chlorophenylbutyrohydroxamic acid and their uses as extracting agents for chromium(vi), molybdenum(vi), titanium(iv) and uranium(vi). A thesis submitted for the Degree of Master of Science in Chemistry Faculty of Science University of Khortoum.

Adebayo, G. P., Oduselu, G. O., Aderohunmu, D. V., Klika, K. D., Olasehinde, G. I., Ajani, O. O. and Adebiyi, E. (2024). Structure-based design, and development of amidinyl, amidoximyl and hydroxamic acid based organic molecules as novel antimalarial drug candidates. *Arab. J. Chem.* **17**(2):105573.

Amtul, Z., Rahman, A. U., Siddiqui, R. A. and Choudhry, M. I. (2002). Chemistry and mechanism of urease. *Curr. Med. Chem.* **(9):** 1323-1348.

Brown, D. A., Errington, W., Glass, W. K., Haase, W., Kemp, T. J., Nimir, H., Ostrovsky, S. M. And Werner, R. (2001). Magnetic, spectroscopic, and structural studies of dicobalt hydroxamates and model hydrolases. *Inorg. Chem.* **40**(9): 5962-5971.

Chauhan, D. S., Verma, K. K., and Garg, S. (2017). Synthesis, characterization and antimicrobial studies on some pyridoxylidene-sulphamethoxazole Schiff base tellurium(IV) complexes. *Der Pharma Chemica.* **9**(8):59-64.

Chauhan, S., Deepak, Garg, S., and Verma, K. K. (2016). Study on 4- methoxybenzohydroxamate complexes of aryltellurium (IV) and diaryltellurium (IV). *Int. j. Chem. Sci.* **14**(1):269-282.

Danah, A., Othman, A., Beatriz, G., Torre, D., Fernando, A. (2020). Hydroxamate siderophores: Natural occurrence, chemical synthesis, iron binding affinity and use as Trojan horses against pathogens. *Eur.J. Med. Chem.* **11**(208): 112-132

Elamin, N. Y., and Ali, E. A. (2021). Preparation, characterization and evaluation of extraction efficiency of Np-tolyl-N benzohydroxamic acid towards certain metal ions. *Asian J. Appl. Chem. Res.* **8**(1): 30-39.

Fischer, M. A., Mustafa, A. H. M., Hausmann, K., Ashry, R., Kansy, A. G., Liebl, M. C. and Kramer, O. H. (2024). Novel hydroxamic acid derivative induces apoptosis and constrains autophagy in leukemic cells. J. Adv. Res. **60**:201-214.

Fugu, M. B. (2019). A Novel di and multi-topic hydroxamate ligands towards discrete and extended network complexes*. A PhD. thesis submitted to School of Natural Sciences Bangor University.*

Fugu, M. B., Coley. J., Dickinson, I. F., Orton, J. B., Klooster, W., Gleesond, M. P. and Jones, L. F.R. (2019). Slight ligand modifications within multitopic linear hydroxamates promotes connectivity differences in Cu(II) 1-D coordination polymers, *CrystEngComm*, 23, 5531-5539.

Gaynor, D. Starikova, Z. A., Haase, W. and Nolan, K. B. (2001). Copper(II) complexes of isomeric aminophenylhydroxamic acids. A novel 'clam-like' dimeric metallacrown and polymeric helical structure containing interlinked unique copper(II) sites. *J. Chem. Soc.* 1578-1581.

Haron, M. J., Jahangirian, H., Yusof, N. A., Kassim, A., Rafiee-Moghaddam, R., Peyda, M., Abdollahi, Y. and Amin, J. (2012). Benzyl and methyl fatty hydroxamic acids based on palm kernel oil as chelating agent for liquid-liquid iron (III) extraction. *Int. J. Mol. Sci.* **13**(4): 2148-2159.

Hassan, K. F., Kandil, S. A., Abdel-Aziz, H. M. and Siyam, T. (2011). Preparation of poly (hydroxamic acid) for separation of Zr/Y, Sr system. *Chromatogr. Res. Int*. **38**(12): 1- 6.

Jarvis, H., Robert, M., Jones, D. and David C. (2023). Discovery of a hydroxylamine-based brain- penetrant EGFR inhibitor for metastatic non-small-cell lung cancer. *J. Med. Chem.* **66**(22): 15477-15492.

Johann, T., Keth, J., Bros, M. and Frey H. (2019). A general concept for the introduction of hydroxamic acids into polymers. *Chem. Sci*. **10**(29): 7009-7022.

Kahn, O. (2000). Chemistry and physics of supramolecular materials. *Acc. Chem. Res*. **3**(33): 647-657.

Kakkar, R. and Gupta, S. (2013). Theoretical studies on hydroxamic acids. *Springer*. **3**(8): 642- 651.

Latifah, R. H., Hadariah, B., Kalavathy, R. and Tajuddin A. M. (2019). Synthesis and characterization of benzohydroxamic acid and methylbenzohydroxamic acid metal co mplexs and their cytotoxicty study. *Malaysian Journal of Analytical Sciences. (MJAS)* **35**(23): 263-273.

Mandeep, D. (2017). A Textbook of inorganic chemistry. *International Edition*. **1**(1):259-270.

Marmion, Celine, J., Griffith, D. and Nolan, K. B. (2004). Hydroxamic acids an intriguing family of enzyme inhibitors and biomedical ligands. *Eur. J. Inorg Chem*. **33**(15): 3003- 3016.

Miller, T. A., Witter, D. J. and Belvedere, S. (2003). Histone deacetylase inhibitors. *J. Med. Chem.* **28**(46): 5097-5116.

Mishra, R. C., Tripathi, R. and Katiyar, D. (2003). Synthesis of new glycosylated b-amino hydroxamates class of antimalarials. *Bioorg. Med. Chem.* **23**(11): 5363-5374.

Ndahi, N. P., Husseini, G., Ibrahim, I., Ahu, A. O. and Habila, A. N. (2018). Complexes of Mn(II) and Fe(II) with Schiff base derived from trimethoprim with salicyldehyde and benzaldehyde as potential antimicrobial agent. *Niger. J. Pharm. Biomed. Res.* **3**(1): 1419-2579.

Patel, P., Shrivastava, S. K., Sharma, P., Kurmi, B. D., Shirbhate, E. and Rajak, H. (2024). Hydroxamic acid derivatives as selective HDAC3 inhibitors: computer-aided drug design strategies. J. Biomol. Struct. Dyn. **42**(1):362-383.

Pepeljnjak, J., jepan, S. T., Zorc., Branka., Butula, I. (2005). Antimicrobial activity of some hydroxamic acids. *Acta Pharmaceutica*. 1**3**(55): 401-408.

Saif, M., El-shafiy, H. F., Mashaly, M. M., Eid, M. F., Nabeel, A. I. and Fouad, R. (2016). Synthesis, characterization, and antioxidant/cytotoxic activity of new chromone Schiff base nano-complexes of Zn(II), Cu(II), Ni(II) and Co(II). *J. Mol. Struct*. 1-42

Santo, L., Hideshima, T., Kung, A. L., Tseng, J. C., Tamang, D., Yang, M., Jarpe, M., vanDuzer, J. H., Mazitschek, R., Ogier, W. C., Cirstea, D., Rodig, S., Eda, H., Scullen, T., Canavese, M., Bradner, J., Anderson, K. C., Jones, S. S. and Raje, N. (2012). Preclinical activity, pharmacodynamic, and pharmacokinetic properties of a selective *HDAC6* inhibitor, *ACY*-1215, in combination with bortezomib in multiple myeloma. *Blood.* **11**(19): 2579-2589.

Sharma, M., Sharma, N. N. and Bhalla, T. C. (2012). Biotransformation of acetamide to acetohydroxamic acid at bench scale using acyl transferase activity of amidase of Geobacillus pallidus BTP-5x MTCC 9225. *Ind. J. Microbiol.* **13**(52): 76-82.

Sow, I. S., Gelbcke, M., Meyer, F., Vandeput, M., Marloye, M., Basov, S. and Dufrasne, F. (2023). Synthesis and biological activity of iron (II), iron (III), nickel (II), copper (II) and zinc (II) complexes of aliphatic hydroxamic acids. *J. Coord. Chem.* **76**(1), 76-105.

Temel, H. (2014). Synthesis and spectroscopic studies of new Cu(II), Ni(II), VO(IV) and Zn(II) complexes with n,n-bis(2-hydroxynaphthalin-1-carbaldehydene)-1,2-bis(o- aminophenoxy) ethane. *J. Coord. Chem.* **57**(9): 723-729.

Tobias, J., Jennifer, K., Matthias, B. and Holger, F. (2019). A general concept for the introduction of hydroxamic acids into polymers. *Chem. Sci.* **29**(11): 10-12.

Tripathi, K., Kumar, N., Singh, M. and Singh, R. K. (2020). Fungal siderophore: biosynthesis, transport, regulation, and potential applications. *Springe.r* **23**(11) 122-124.

Wazir, I. (2022). Water-soluble lanthanide cupferron type complexes as palliative for bone cancer treatment. Thesis submitted in fulfillment of the requirements for the degree of Doctor of Philosophy in Chemistry in the Faculty of Science at the University of Johannesburg South Africa.

Waziri, I., Wahab, O. O., Mala, G. A., Oselusi, S. O., Egieyeh, S. A. and Nasir, H. (2023). Zinc II complex of (Z)-4-((4-nitrophenyl) amino) pent-3-en-2-one, a potential antimicrobial agent: Synthesis, characterization, antimicrobial screening, DFT calculation and docking study. *BCSE* **37**(3):633-651.